RESULTS FROM SOME TEMPERATURE MAPPING EXPERIMENTS ON Nb_3Sn RF CAVITIES

P. Boccard[1,2],P. Kneisel[1],G. Müller[3],J. Pouryamout[3] and H. Piel[3]

[1]Thomas Jefferson National Accelerator Facility
Newport News, Virginia, USA

[2]Old Dominion University, Norfolk, Virginia, USA

[3]Bergische Universität Wuppertal, Fachbereich Physik
D 42097 Wuppertal,Germany
and
Cryoelectra GmbH, D-42287 Wuppertal, Germany

Abstract

In a previous paper [1] we reported about the performances of several high purity niobium cavities which had been coated with a Nb3Sn layer by the vapor diffusion process. These cavities performed quite well, showing low residual surface resistance values in the nohm range and peak electric surface fields above 25 MV/m with little electron loading. However, a rather strong dependence of the Q-value on field gradient in the cavity was observed. We have applied a rotating temperature mapping system to some of these cavities during re-testing and acquired temperature maps in subcooled helium at different field levels in the cavities. Three different types of heating distributions were found: a broad area heating along an azimuth caused by trapped magnetic flux generated by thermocurrents, localized heating due to a defect, and homogeneous heating over the whole cavity surface.

I. Introduction

In previous work [1], a vapor diffusion technique has been optimized for coating high purity Nb 1.5 GHz cavities with Nb_3Sn. The improved technique has resulted in cavities which maintain a high thermal stability with respect to defects. Q_0 values of up to 10^{11} at 2 K and 10^{10} at 4.2 K have been obtained. These cavities marked the first time residual resistances of less than 10 $n\Omega$ were reproducibly achieved for Nb_3Sn surfaces.

With respect to high field performance, these cavities show little electron loading up to peak electric surface fields of 25 MV/m. However, these cavities do show a strong

dependence of Q_0 on the field gradient at high fields. At 2 K (4K), Q_0 is nearly constant up to a peak field of about 15 MV/m from which it degrades to about 10^9 at 30 (25) MV/m.

To investigate the loss mechanisms causing this Q_0 degradation, we have applied the technique of temperature mapping [2] in subcooled helium to the outer surface of some of these cavities. With this technique we were able to identify the distribution of RF losses. In addition, the mapping was a useful probe of the local surface resistance which allowed us to make qualitative comparisons between the localized losses and global losses measured by Q(E) curves.

II. Experimental Method

The mapping of the cavity surface is achieved with the use of a rotating arm as shown in Figure 1. The arm is connected to a gear which is driven by a motor at the top of the test stand which allows the thermometers to be rotated to various positions. The arm holds 16 thermometers which are positioned along the curved section of the cavity surface. The beam tubes are not mapped. Each thermometer is an Allen Bradley 100 Ω 1/8 watt resistor which is mounted at the end of a flexible G10 finger. The resistor makes direct contact with the cavity surface.

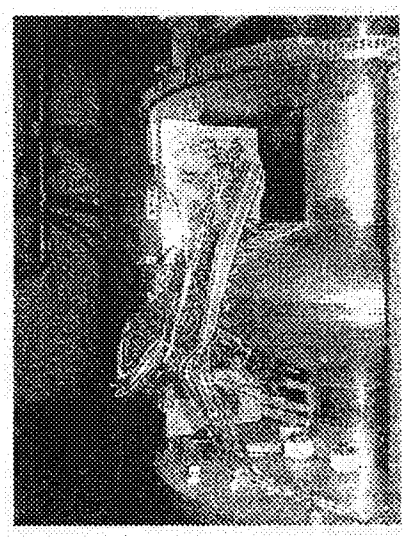

Figure 1: Scanning apparatus for temperature mapping of cavity surface.

The data acquisition is done using a Macintosh IIx computer controlled through a LabView program and a custom scanning electronics originally developed for calorimetry measurements in a triaxial cavity [3,4].

Two types of temperature maps were acquired. The first consisted of mapping the entire surface of the cavity. In this case, the RF power was first applied to the cavity and the temperature read on each of the sensors. Then the power was turned off and the temperature was read again. This allowed us to determine ΔT for each sensor. Subsequently, the arm was rotated to a new position and the pulsing procedure repeated. Nominally, the data were taken at 12 degree intervals. In the second type of test, a similar

procedure was followed except the arm remained at one position and the field level in the cavity was changed.

The scans were performed in subcooled helium since early tests indicated that our temperature sensors were insensitive in superfluid helium or at 4.2 K; in both cases no RF heating signal could be obtained. Subcooled experiments are well suited to experiments on Nb_3Sn surfaces since the T_c is 18.2 K, putting us well into the region of the temperature independent residual resistance. In our experiments the bath temperature typically drifts from 2.2 - 3.0 K over the course of three to four scans, each taking approximately 30 minutes. The error in the ΔT signal is due to fluctuations in the bath temperature, cooling conditions at the sensor and variation in the contact between the sensor and the cavity wall. The error is estimated to be on the order of 10%.

III. Results

In all, three cavities were tested in this investigation. The cavities had Q_0's at 4.2 K better than 10^9 out to a peak E field of 12 MV/m. Typically, we achieved a Q_0 at 2 K of about 10^{10} out to 15 MV/m. Note that in these cavities the relationship between E_{peak} and the maximum surface B field is $B_{peak}/E_{peak} = 25.8$ gauss/(MV/m).

Figure 2 shows the Q(E) curve for our best cavity. Each cavity's Q(E) curves share a similar appearance. The general features are a small linear degradation of the Q at low peak E fields followed by a plateau region for fields up to 12-18 MV/m at which point there appears a stronger exponential degradation in the Q. During the measurements of Q_o vs. E_{peak}, electron loading was sometimes detected at very high fields which occasionally triggered a quench of the cavity, but was not responsible for the Q degradation at high fields.

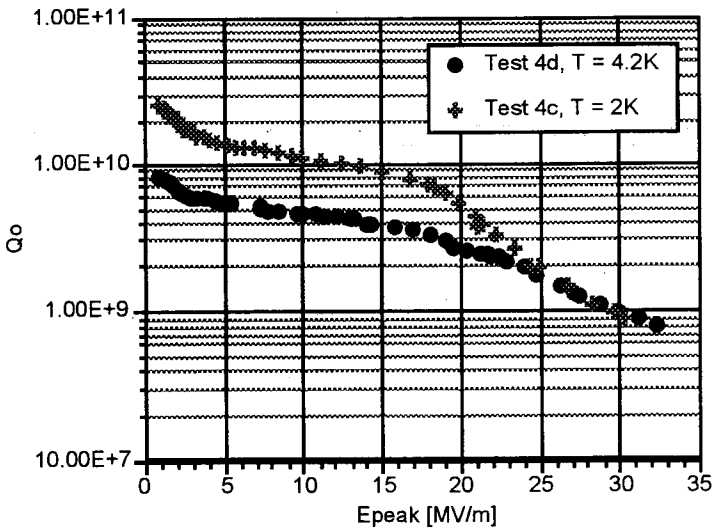

Figure 2: Q vs. E_{peak} dependence for the best Nb_3Sn cavity. One can clearly see three different sections, which are universal for all tested Nb_3Sn cavities in this investigation: for $E_{peak} < 3$ MV/m Q_o decreases linearly with field, for $4\,\mathrm{MV/m} \le E_{peak} \le 17\,\mathrm{MV/m}$ a plateau region appears, followed by an exponential decrease of Q with field at larger E_{peak}.

In Figure 3, the effect of quenches on the cavity Q_0 is shown. After several quenches, the Q has degraded by a factor of 2 or 3. This degradation was reversible. After warming the cavity above T_c and recooling, the original Q(E) performance was restored.

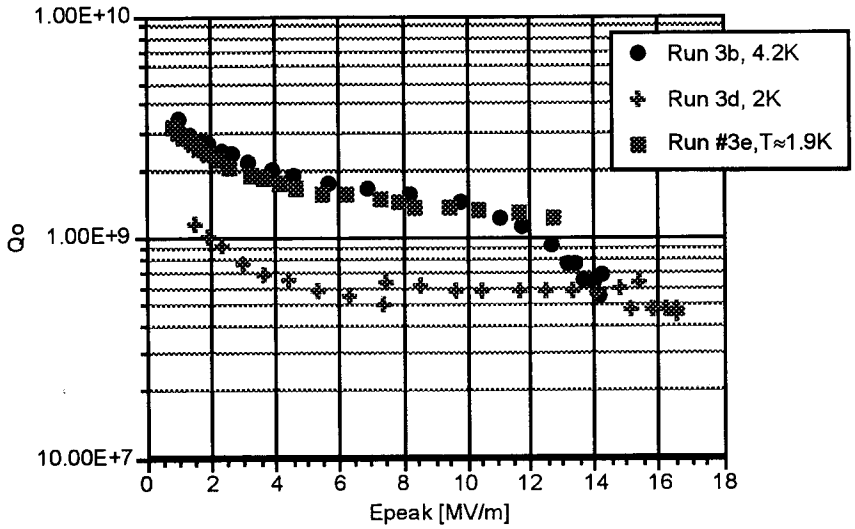

Figure 3: Q vs. Epeak curves for cavity 3 showing the effect of quenches. Run 3b was taken before the cavity quenched. Run 3d was taken after several quenches had degraded the Q. For Run 3e, the cavity was warmed up past Tc and recooled, which improved the performance.

We took temperature maps on all three cavities and found the maps can be categorized into three different types: 1) broad area heating along an azimuth, 2) localized heating, and 3) homogenous heating over the whole surface.

Figure 4 shows a distribution which was a broad heating peak along an azimuth of cavity 1. The longitudinal extent was nearly the length of the entire cavity. The width of the peak at its half maximum covered over 1/4 of the cavity's surface. Increases in the field led to larger heating ΔT's and the response of the thermometers at the maximum heating azimuth appears to be a linear function of E^2 (Figure 5) over the whole range of fields tested. Thus, this map does not reflect the increased losses seen in the Q(E) curve. The additional losses may come from other areas of the cavity. The data from three full cavity temperature maps at 3.3, 8.1, and 10.3 MV/m has also been analyzed. Along the azimuth of maximum heating, there was again a nearly constant surface resistance. However, at an azimuth away from the broad heating peak, the surface resistance was increasing with the field in agreement with the Q(E) data.

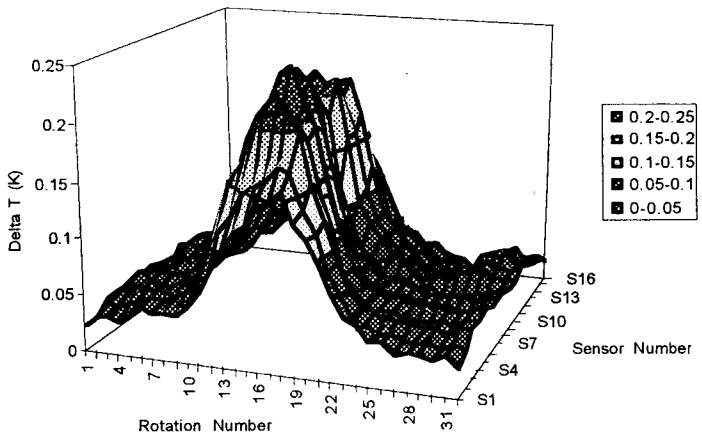

Figure 4: Full cavity temperature map of cavity 1 at Epeak = 8.1 MV/m showing a broad heating area along an azimuth.

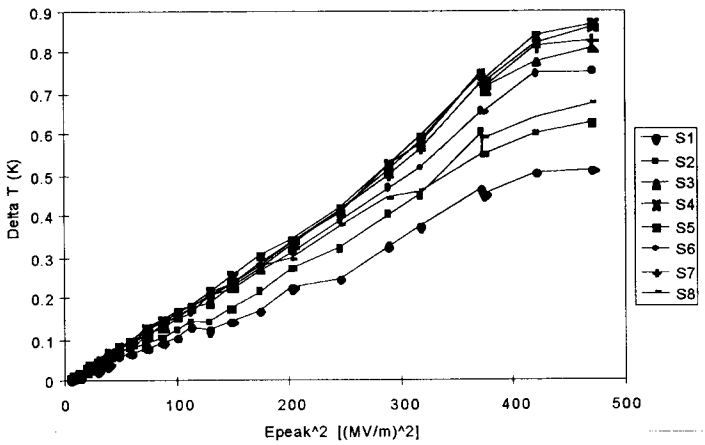

Figure 5: Temperature map for cavity 1 along azimuth of maximum heating. At high fields the thermometry appears to be saturating.

A very similar distribution, as shown in Figure 6, was found on cavity 3 after a few quenches had lowered the Q value (see also Figure 3). After warm up of the cavity and recooling, the broad heat distribution disappeared.

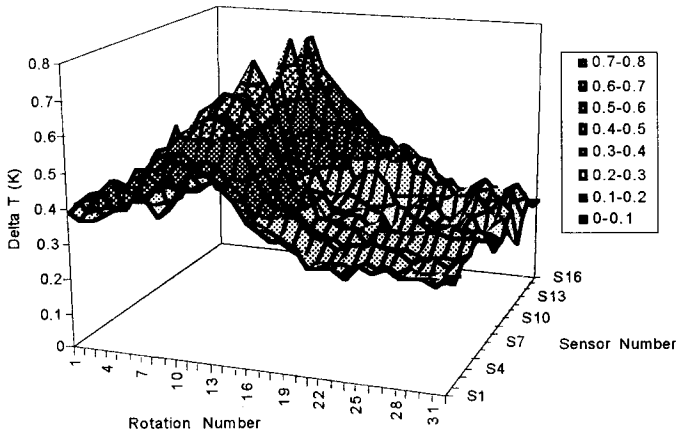

Figure 6: Full cavity temperature map of cavity 1 at E_{peak} = 15.4 MV/m showing broad heating area along an azimuth after several quenches had degraded the Q.

Figure 7, a map taken on cavity 2 at E_{peak} = 4.2 MV/m, shows losses which were more localized indicating the presence of a defect. The azimuthal range was about 30 degrees, while the longitudinal extent was 3-4 thermometer positions. The heating peak was located along the bottom half of the cavity. A temperature map at the azimuth of the defect as a function of field level (Figure 8) showed the response changed at a field level of about 6 MV/m while a similar map taken about 90 degrees away, the heating was too small to be seen with our thermometry below 5 MV/m. At higher fields, the losses increase less rapidly near the defect than in the map 90 degrees away which might indicate that our thermometers are saturating at high heating levels.

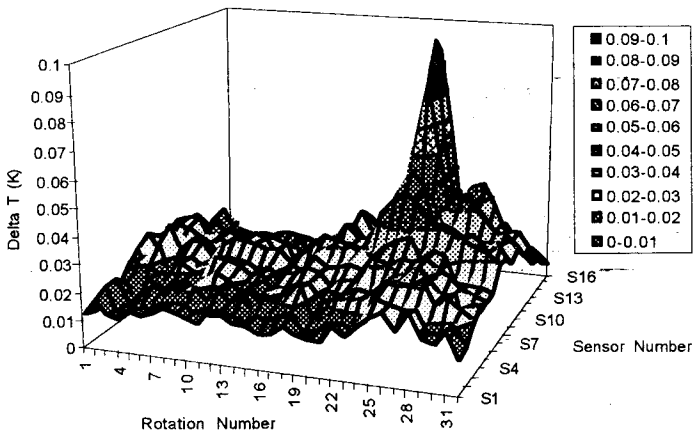

Figure 7: Full cavity temperature map of cavity 2 at E_{peak} = 4.2 MV/m showing a localized heating area due to a defect.

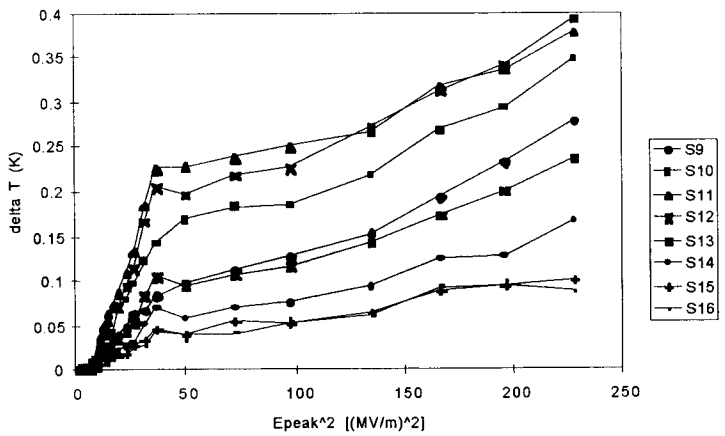

Figure 8: Temperature map for cavity 2 along azimuth of maximum heating for sensors 9 through 16 as a function of E^2_{peak}.

Figure 9, a map taken on cavity 3 at E_{peak}= 9 MV/m, shows the rather homogeneous heating of the whole cavity surface. This rather uniform heating is changing at higher fields as can be seen by comparing Figure 9, taken in the "plateau" region, to Figure 10 (E_{peak}= 18.3 MV/m) taken in the Q degradation region (see Figure 2). Both maps show a more pronounced heating of the lower half of the cavity, possibly indicating poorer cooling conditions there.

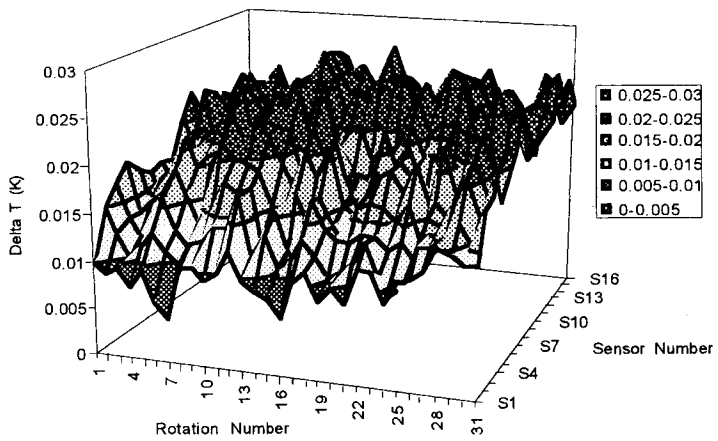

Figure 9: Full cavity temperature map of cavity 3 at E_{peak}= 9 MV/m, in the plateau region of the Q(E) curve, showing broad heating of cavity surface.

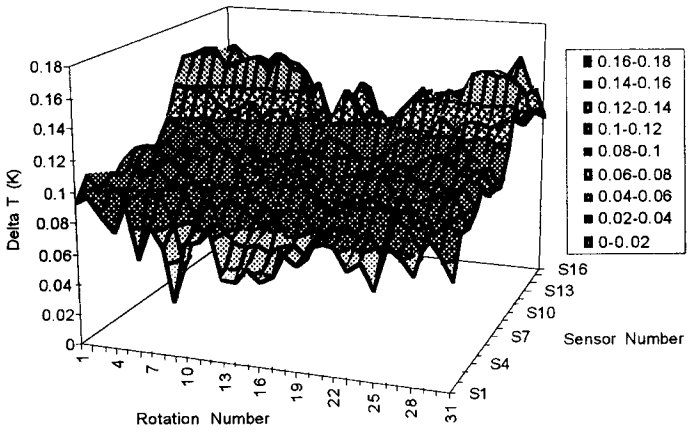

Figure 10: Full cavity temperature map of cavity 3 at E_{peak}= 18 MV/m, in the high field Q degradation region, showing broad heating of cavity surface which has changed with respect to the map at 9 MV/m in Figure 9.

A temperature map at fixed azimuth (Figure 11), appears to show a linear dependence in E^2 up to fields of 14 MV/m. To investigate this further, we plotted $\Delta T / E^2_{peak}$ vs. E_{peak} in Figure 12. Below 4 MV/m the surface resistance, which $\Delta T / E^2_{peak}$ is a measure of, is increasing as expected from the decreasing Q value. Between 4 and 14 MV/m, we do not see any changes in the surface resistance. This may indicate that the losses responsible for the slight Q degradation in the plateau region are located in another region of the cavity.

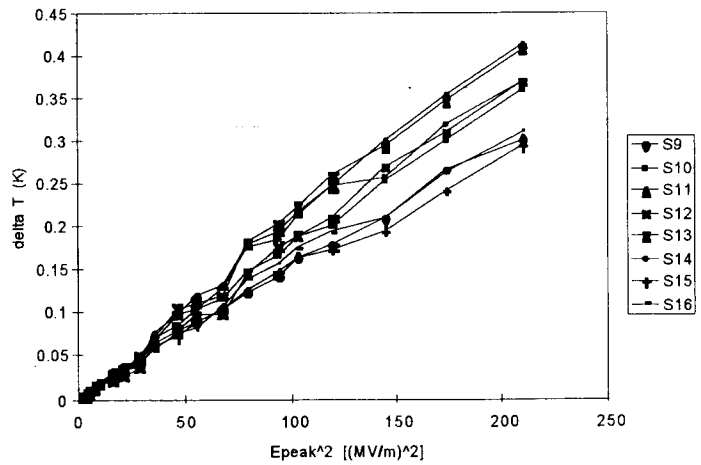

Figure 11: Temperature map for cavity 3 for sensors 9 through 16 as a function of E^2_{peak}. The plot is linear in E^2_{peak} as expected from a constant surface resistance. Note that this map only extends through the plateau region of the Q(E) curve.

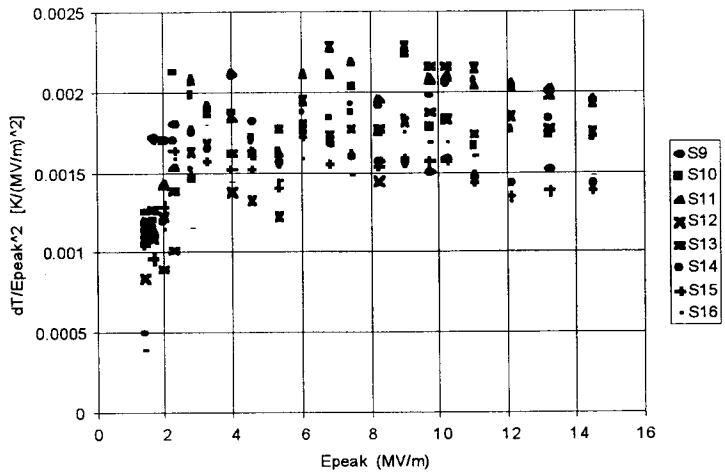

Figure 12: $\Delta T/E_{peak}^2$ vs. E_{peak}. This plot is a measure of the local surface resistance as a function of the field. At low fields the resistance is increasing as expected from the Q(E) curve.

IV. Discussion

The best Q(E) performance resulted in Q_0 values at 4.2 K $> 3 \times 10^9$ out to peak E fields of 15 MV/m, which exceeds the design goal of CEBAF. We reached an E_{peak} of 32 MV/m, the highest value ever obtained in a Nb_3Sn cavity. However, due to the exponential decrease in the Q-value above 15 MV/m our Q was only 8×10^8. This eliminates Nb_3Sn technology for such high gradient applications as TESLA, but it may be applicable for future accelerator applications with somewhat more modest design goals for the accelerating gradient if similar results can be achieved in multicell cavities and if slow cooldown at 18 K and quench avoidance can be realized. Fast cooldowns have been shown to degrade the Q values due to extra losses from thermally induced currents [5].

Initial Q degradation was seen in all of our Q(E) tests. These low field losses are believed to be due to flux penetration into weak links which saturates at medium field levels [5]. We have seen these low field losses with thermometry in cavity 3 which had homogeneous heating. In cavity 2, the losses were seen but may have been the result of the localized defect. In a region away from the defect the losses were too low at low fields to be seen with our thermometry. In cavity 1, the low field losses were not seen by the thermometry but may have been masked by the losses due to the frozen in flux.

The high field losses past the plateau region do not appear to be the result of field emission. The Q(E) curves suggest that the surface resistance is increasing in this region. However, we did not see this well pronounced in our fixed azimuth map for cavity 1, presumably due to saturation effects in the thermometers ($\Delta T \cong 1K$). This saturation might be caused by the additional losses due to trapped flux. Cavity 2 temperature maps showed increasing surface resistance as well but the increases were faster in regions away from the defect, again indicating saturation effects. According to full cavity temperature maps for cavity 3, the high field losses are broadly but not uniformly distributed over the cavity surface. Thus high field losses may be the result of broad regions of increasing surface resistance. The apparent saturation in the thermometry suggests that superfluid thermometry may be necessary to study the high field losses in these cavities.

The onset field of the high field Q degradation was similar in all three cavities. This may be pointing to some fundamental loss mechanism which is occurring above the expected H_{C1} of the Nb_3Sn layers.

The occurrence of quenches shows that the cavities have not been sufficiently stabilized against thermal defects. This is a crucial point since the Q of the cavity degrades throughout the whole field range after these quenches. The temperature maps indicate that the losses due to these quenches are broadly distributed and quadratic in the field (i.e. a constant surface resistance). Since the additional losses are removed by warming up the cavity past its critical temperature and recooling, this strongly suggests they are due to frozen in flux caused by thermocurrents.

Acknowledgments

Many thanks to P. Kushnick for his support in cryogenic operations during these experiments.

This work was supported by the U.S. DOE under contract number DE-AC05-84ER40150.

References

[1] G. Müller,P. Kneisel, D. Mansen, H. Piel, J. Pouryamout, and R.W. Röth , Proc. of the 5th EPAC, London, p.2085 (1996).

[2] H. Piel, Proc. of the Workshop on RF Superconductivity, KfK Report 3019, 85 (Kernforschungszentrum Karlsruhe 1980).

[3] C. Liang, L. Phillips, and R. Sundelin, Rev. Sci. Instrum. **64**, 1937 (1993).

[4] C. Liang, Ph.D. Thesis, Virginia Polytechnic Institute and State University, (1993).

[5] M. Peiniger, M. Hein, N. Klein, G. Müller, H. Piel, and P. Thuns, Proc. of the 3rd Workshop on RF Superconductivity, Argonne, ANL-PHY-88-1, 503 (1988).